

Acoustic emission-based indicators of shear failure of reinforced concrete beams without shear reinforcement

Zhang, Fengqiao; Yang, Yuguang; Hendriks, Max A.N.

DOI

10.1016/j.engstruct.2025.119929

Publication date

Document Version Final published version

Published in **Engineering Structures**

Citation (APA)

Zhang, F., Yang, Y., & Hendriks, M. A. N. (2025). Acoustic emission-based indicators of shear failure of reinforced concrete beams without shear reinforcement. *Engineering Structures*, *330*, Article 119929. https://doi.org/10.1016/j.engstruct.2025.119929

Important note

To cite this publication, please use the final published version (if applicable). Please check the document version above.

Copyright

Other than for strictly personal use, it is not permitted to download, forward or distribute the text or part of it, without the consent of the author(s) and/or copyright holder(s), unless the work is under an open content license such as Creative Commons.

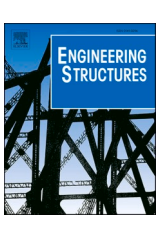
Please contact us and provide details if you believe this document breaches copyrights. We will remove access to the work immediately and investigate your claim.

ELSEVIER

Contents lists available at ScienceDirect

Engineering Structures

journal homepage: www.elsevier.com/locate/engstruct



Acoustic emission-based indicators of shear failure of reinforced concrete beams without shear reinforcement

Fengqiao Zhang ^{a,*}, Yuguang Yang ^a, Max A.N. Hendriks ^{a,b}

- a Department of Engineering Structures, Delft University of Technology, Delft 2628CN, the Netherlands
- b Department of Structural Engineering, Norwegian University of Science and Technology, Trondheim 7491, Norway

ARTICLE INFO

Keywords: Shear failure indicator Acoustic emission monitoring Reinforced concrete structures Strut and tie Structural assessment

ABSTRACT

Many existing concrete structures require effective assessment of the bearing capacity. A critical failure mode is shear, especially for concrete structures without or with limited shear reinforcement. The shear failure is brittle and often leads to loss of property and lives. Therefore the shear failure should be indicated before it occurs. A potential solution is to use acoustic emission (AE) monitoring, which is sensitive to minor changes in concrete, even micro-cracking, both on the surface and inside the structure. By combining the knowledge of shear failure processes and AE techniques, this paper presents an AE-based shear failure indication system. The system automatically identifies three levels of structural damage levels up to shear failure, which are categorized from minor to severe levels as green-light, yellow-light, and red-light criteria. The 'traffic light system' is validated using six shear tests on full-scale reinforced concrete beams without shear reinforcement. The robustness of the system is also validated across these tests.

1. Introduction

The safety of existing concrete structures is crucial for society. Many existing structures built in the 1960s and 1970s were designed according to the past codes which are now considered deficient by the current codes [1,2]. Moreover, the aging of material over time leads to a further reduction in structural bearing capacity. Meanwhile, the load applied to the bridges increases due to heavier traffic. Outdated design details, aging materials, and increasing loads may lead to structural failure.

A critical type of failure for concrete structures is shear, especially for those without or with limited shear reinforcement [3]. Shear failure is brittle, thus hard to be detected before it occurs [4]. The consequence of shear failure is catastrophic, which could be loss of properties and lives.

To prevent shear failure, effective assessment of the bearing capacity against shear is needed. Two methods are usually applied for structural assessment: proof load testing [5] and long-term monitoring [6]. In both cases, information of structural behaviour is needed. In the case of shear failure of reinforced concrete without shear reinforcement, the critical information is related to the crack location and magnitude [7–11].

Many monitoring techniques can be used to obtain the crack information, such as Linear Variable Differential Transformers (LVDT) [6], strain gauge [12], Digital Image Correlation (DIC) [13], Fibre Optical

Sensors (FOS) [14], Ground Penetration Radar (GPR) [15], Infrared Thermography (IR) [16], Radiography [17], Ultrasonic pulse velocity (UPV) [18], Impact echo (IE) [19], Acoustic Emission (AE) [20], etc. These techniques have their pros and cons for the purpose of monitoring concrete cracking. Some techniques such as LVDT and DIC are only suitable for monitoring concrete surface cracking, losing the information of internal damages which could be critical for shear failure. Some techniques such as GPR, Radiography and UPV require active measurement. In the case of low measurement frequency, these techniques cannot detect the crack development in real time, which will influence the timely decisions regarding the shear failure.

Among these techniques, AE stands out for its promising features: it can detect not only surface cracking but also internal cracking; it is sensitive to minor changes in concrete even microcracking [21] so that the crack detection can be at an early state; it can serve for near real-time monitoring; moreover, AE sensors are easy to install on the structural surface. By combining the knowledge of AE and shear failure, we aim to develop AE-based shear failure indicators.

We begin by reviewing the theoretical shear failure process in reinforced concrete structures without shear reinforcement. A critical failure mode is selected for assessment: flexural shear failure, where shear capacity is determined by the shear transfer mechanisms along the flexural

E-mail address: F.Zhang-5@tudelft.nl (F. Zhang).

^{*} Corresponding author.

shear crack. The theoretical review motivates a potential indicator for flexural shear failure, which is the damage level of the strut. The strut refers to the compressive field between the load and the support. Then, we monitor the strut damage condition using AE. A recently proposed AE data analysis method by the authors is applied. This method computes a parameter called the probability density field of AE events (pdAE), which quantifies the spatial distribution of AE events more realistically. In a previous study, we found that pdAE is related to crack kinematics, including crack width and shear displacement, depending on the location of the crack. We use pdAE to evaluate the damage level of the strut as an indicator of the flexural shear failure.

Based on this evaluation, we propose an AE-based indication system that can automatically identify three levels of structural damage before shear failure of reinforced concrete beams without shear reinforcement. These levels are categorized from minor to severe damages as greenlight, yellow-light, and red-light criteria. The proposed shear failure indicators are validated using experimental data from six full-scale shear tests. These indicators can support structural assessment in both proof load testing and long-term monitoring.

2. Integrity of strut as a shear failure indicator

Understanding the shear failure process is essential for developing a reliable indicator. According to the mechanical models of shear failure in reinforced concrete structures without shear reinforcement [7–11], the process begins with the formation of flexural cracks. As the shear force increases, the inclination of the flexural cracks also increases, and the dowel crack begins to open from the bottom of the existing flexural crack (Fig. 1). At this stage, due to the larger crack width, the contribution from aggregate interlock reduces. At a certain shear force, a flexural shear crack forms. Then, depending on whether the flexural shear crack damages the strut which is an estimated compressive region between the load and the support as marked in Fig. 1, the shear capacity of the structure varies.

For an uncracked strut, the structural shear capacity is often higher, determined by the concrete compressive strength (shear compression failure). For a cracked compressive strut, the capacity is lower, determined by shear transfer mechanisms along the flexural shear crack (flexural shear failure) [22]. The shear failure process highlights the importance of the integrity of the strut to the shear capacity of reinforced concrete structures without shear reinforcement.

Compared to shear compression failure, flexural shear failure generally results in a lower shear capacity and is therefore more critical for this type of structure. This paper focuses on identifying flexural shear failure.

3. Probability density field of AE events and its relationship with crack kinematics

To effectively monitor the integrity of the strut, an appropriate technique should: (1) be sensitive to internal concrete cracking, as the strut region is located within the structure, (2) be capable of performing full-field measurements, since the crack location in the strut is not always predictable, (3) be easy to install both in the lab and on-site, and (4) provide near real-time monitoring so that timely interventions can be taken as needed.

AE fulfils the above requirements due to its working principle. Sudden changes in concrete like cracking even microcracking will release energy and generate waves. The waves will propagate from the source location to the sensor location on the structural surface. By processing the received signals at sensors, AE can estimate the location of the sources which do not need to be at the location of sensors but also can be inside the structure. This process is called source localization [23]. In AE monitoring, sensors are installed on the structural surface thus easy to install. And the signals from the cracking can be acquired and processed time-efficiently, therefore giving near real-time data.

However, AE source localization can only estimate the location of the cracking activities, but provides limited information on crack kinematics, such as the crack width and shear displacement. These are essential information to indicate the damage level of the strut.

To relate AE data to crack kinematics, the spatial distribution of AE events must be properly quantified. We recently proposed an AE data analysis method that calculates a parameter called the probability density of AE event locations (pdAE) to quantify this spatial distribution [24]. The parameter pdAE accounts for various uncertainties in the AE source localization process, such as arrival time picking errors, presence of crack, and sensor locations. The resulting localization error (the distance between the actual and estimated source locations) was evaluated, and based on the error characteristics, the probability of AE event locations was estimated. Fig. 2 exemplifies the localized AE events from a beam test when two cracks opened (CR1 and CR2) and the pdAE field, which more clearly identifies the crack pattern. This example is taken from beam test which is introduced in Section 5.1.

The parameter pdAE was further related to the crack kinematics, depending on the crack location in a beam according to our study reported in a previous paper [25]. Fig. 3a shows the pdAE-crack width relationships with each dashed line measured at a location along a crack. The locations of these measurement can be found in the previous paper. Fig. 3b shows the crack opening history at those measured locations. Fig. 3c illustrates the locations in a beam and the contact area between the two crack faces. The data presented in these figures were obtained from the same tests presented in this paper (in Section 5.1).

We experimentally found two types of pdAE-crack kinematics relationships. Type I relationships usually occur in the tensile zone of a structure, where the crack first opens perpendicular to the crack face and then shear displacement occurs. Due to larger crack width, the contact area between the two crack faces during shear displacement is smaller, resulting in fewer AE events. Type II relationships mostly occur in the compressive zone of a structure, where shear displacement occurs at the beginning of cracking when the crack width is small. The contact area during shear displacement is larger, resulting in more AE events. These results indicate that pdAE is not only related to a single variable, such as

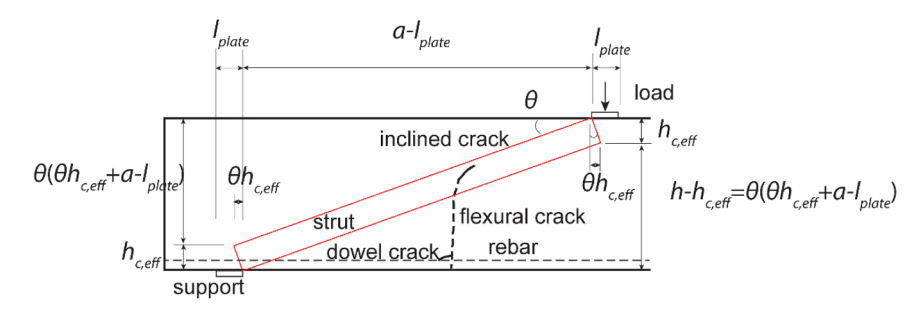


Fig. 1. Formation of the flexural shear crack: development of the inclined crack and the dowel crack from the flexural crack. The determination of the geometry of the strut is indicated.

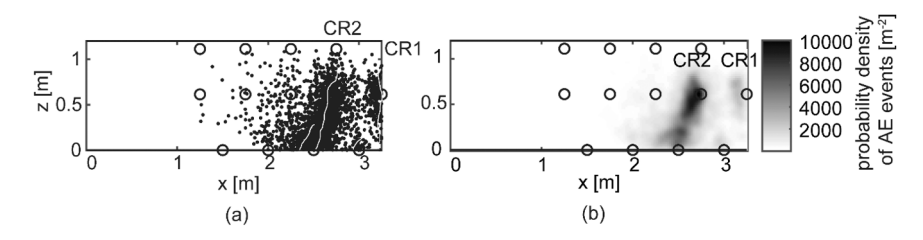


Fig. 2. Demonstration of the pdAE field: (a) localized AE events from concrete cracking CR1 and CR2, and (b) the pdAE field of the localized AE events. (The figure is taken from [24].).

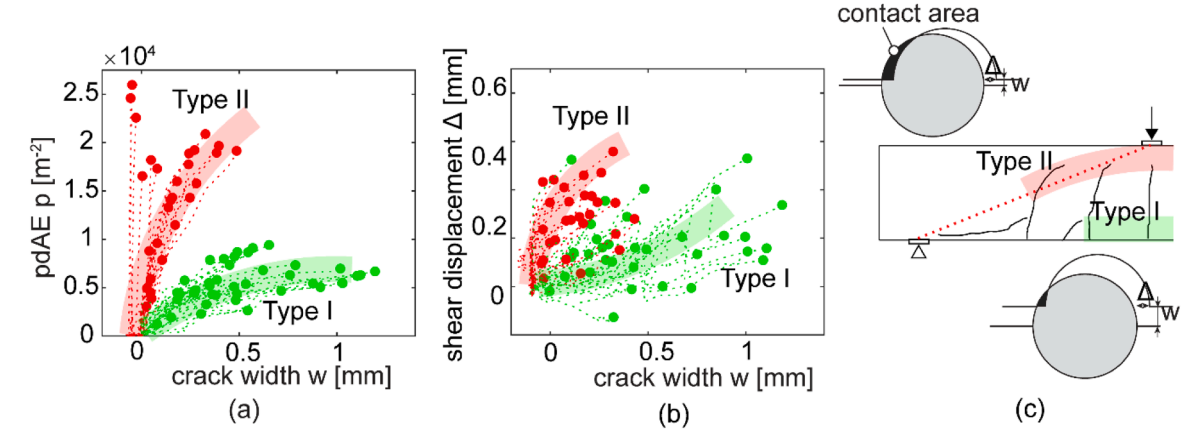


Fig. 3. Relationship between AE events and crack kinematics in Type I and Type II: (a) pdAE-crack width, (b) crack opening history and (c) locations with illustration of contact area. (The figure is taken from [25].).

crack width or shear displacement; rather, it is connected to the full kinematics of the crack.

4. 'Traffic light system' to indicate shear failure

Combining the AE methods and the knowledge of shear failure process in reinforced concrete structures without shear reinforcement, we evaluate the strut integrity using the pdAE, which is developed as a shear failure indicator. In the strut region, the pdAE increases with the crack width following the Type II relationship (Fig. 3), so the maximum pdAE in that region reflects the maximum crack width, representing the damage condition of the strut. As the load increases, the strut becomes more damaged, leading to an increase in the maximum pdAE. When near shear failure, one of the flexural crack develops into a critical flexural shear crack in the strut [26,27], which is usually accompanied by large shear displacement along the crack, resulting in a significant increase in pdAE. Fig. 4b illustrates the increase in pdAE in the compressive strut

with load using a red line.

Then, we automate the evaluation of the strut integrity by taking an AE reference. This reference is taken as the maximum pdAE in the tensile region of the same structure. In the tensile zone, the pdAE increases with the crack width following the Type I relationship (Fig. 3), so the AE reference reflects the maximum crack width in the reference region. As the load increases, the crack width also increases, leading to an increase in the AE reference until the two crack faces no longer make contact. Fig. 4b illustrates the increase in pdAE in the tensile region with load using a green line.

Fig. 4a illustrates the strut region and the reference region. The strut region takes on an idealized prismatic shape. The width of a prismatic compressive strut is determined by the loading plate dimension and the height of the equivalent concrete tensile tie. The determination of the geometry is indicated in Fig. 1. According to the Eurocode [17], the height of the equivalent concrete tensile tie for specimen under bending is given by $h_{c.eff} = \min\{(h-x_c)/3, 2.5(h-d)\}$, where h is the height of

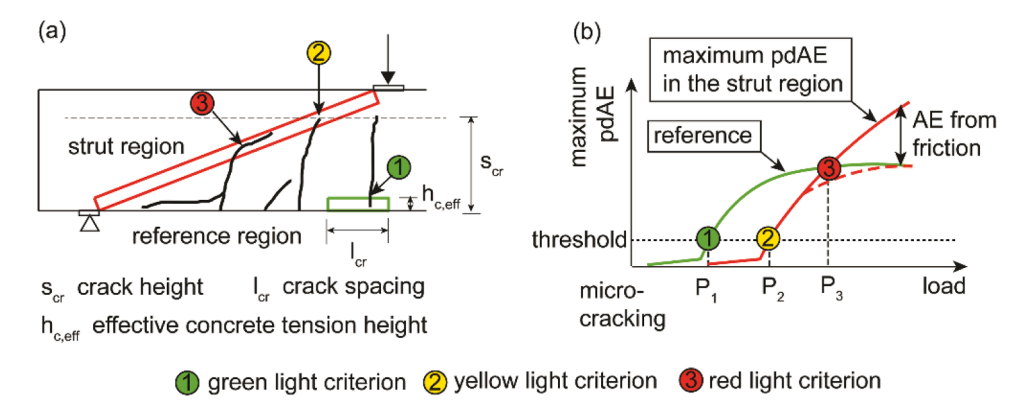


Fig. 4. The traffic light system for shear failure indication: (a) cracking behaviour at the criteria and (b) determination of the criteria by comparing the maximum pdAE in the strut and the reference region.

cross section, x_c is the compressive zone height, d is the effective cross section height. The reference region has a height of $h_{c,eff}$ and a length equal to the estimated flexural crack spacing $l_{cr} = \left(1 + \rho_l n_e - \sqrt{1\rho_l n_e + (\rho_l n_e)^2}\right) d/k_c$, where ρ_l is the reinforcement ratio, n_e is the elastic modulus ratio between steel and concrete, and k_c is the inclination of the stress line [28]. We use a length of one crack spacing to ensure that at least one flexural crack can be covered by the region. The estimated region of strut and tie may deviate from the actual ones, which is

acceptable since the strut and tie model is based on a lower-bound

approximation of the actual load bearing mechanism [19].

The benefits for selecting this reference are as follows:

- For reinforced concrete members without shear reinforcement, under regular loading conditions, the tensile chord with the maximum bending moment will always crack first. Therefore, the pdAE in the tensile chord first shows the sign of cracking and can be used as a reference to indicate the cracking in the compressive strut which occurs later.
- Taking the reference from the same structure avoids the influence of uncertainties related to the structural type, material property, AE setup and environmental noise.
- The reference is taken near the surface of the structure, where the crack pattern can be easily calibrated using observations or other displacement measurements like LVDTs.
- The pdAE in the reference region mainly come from flexural cracking. Other mechanisms, like bond slip or yielding of reinforcement, have been found to have limited influence on the obtained pdAE for structures with a large bulk of concrete.

By comparing the maximum pdAE in the strut to the AE reference, we can identify three structural damage levels up to the flexural shear failure (Fig. 4b). We propose a 'traffic light system' concept to describe these three levels:

- Green-light criterion: the onset of AE reference. This criterion indicates the formation of flexural cracks in the reference region (Fig. 4a). The onset of AE reference is determined when an obvious increase in pdAE is found in the reference region (Fig. 4b). The value of the AE reference at this criterion is used as a threshold for crack initiation in the strut.
- Yellow-light criterion: the maximum pdAE in the strut region exceeds the threshold for crack initiation obtained from the green-light criterion (Fig. 4b). The yellow-light criterion indicates the initiation of the first crack in the strut (Fig. 4a).
- Red-light criterion: the maximum pdAE in the strut region exceeds that in the reference region at the same load level (Fig. 4b). This criterion is usually observed at the critical flexural shear cracking in the strut (Fig. 4a), where larger shear displacement occurs at relatively small crack width, leading to more AE events from friction. The red-light criterion, which indicates the development of a critical flexural shear crack in the strut, is close to failure of both the strut and the entire structure.

It is important to note that when comparing the pdAE in the strut and the reference region, for a given value of pdAE, the crack width in the strut region is typically smaller due to different pdAE-crack width relationships, as illustrated in Fig. 3.

5. Experimental validation of the AE-based 'traffic light system'

The 'traffic light system' proposed in this paper is validated by six shear tests on full-scale reinforced concrete beams without shear reinforcement [29]. They are named as H601A, H602A, H603A, H604A,

H851A and I123A. Fig. 5 shows photos of the test setup and the sensors.

5.1. Description of the experiments

The dimensions of the beams are $10000~\text{mm} \times 300~\text{mm} \times 1200~\text{mm}$. A commercial concrete mixture with strength class C65 is used. Only longitudinal reinforcements were present at the outer layers where the tensile and compressive stress are maximum. Between the longitudinal reinforcement layers, only bulk unreinforced concrete presents.

The beams were simply supported with a span of 9000 mm which was the distance between the centres of the two supports. The beams were loaded by a single point load. The distance between the centre of the point load and the closer support (defined as shear span) was one of the main variables, which was between 3000 mm and 4500 mm. The load was applied through a hydraulic jack in a displacement-controlled manner. Fig. 5a is a photo of the test setup including the beam, loading frame, supports and hydraulic jack.

Table 1 lists the essential configurations of the listed tests, including concrete cubic compressive strength $(f_{c,cube})$ at a certain age, rebar configuration, rebar characteristic yield strength (f_{yk}) , reinforcement ratio (ρ_l) , shear span (a), effective depth (d), shear span ratio (a/d) and load type.

AE sensors of type R6I from MISTRAS [30] were applied to monitor the cracking behaviour. The central frequency is 60 kHz. The sensor was fixed to the specimen by a steel holder (Fig. 5b). The couplant between the sensor surface and structural surface is grease-like material from MOLYKOTE [31]. The data acquisition system is MISTRAS Sensor Highway II.

Fig. 6 shows the AE sensor layouts. The sensors on the side surface are marked in circles and the ones on the bottom surface are marked in rectangles. The sensors on the bottom surface were in the middle line of the width direction. The sensor spacing in the length and height directions were around $0.5 \, \text{m}$, with minimum $0.45 \, \text{m}$ and maximum $0.75 \, \text{m}$.

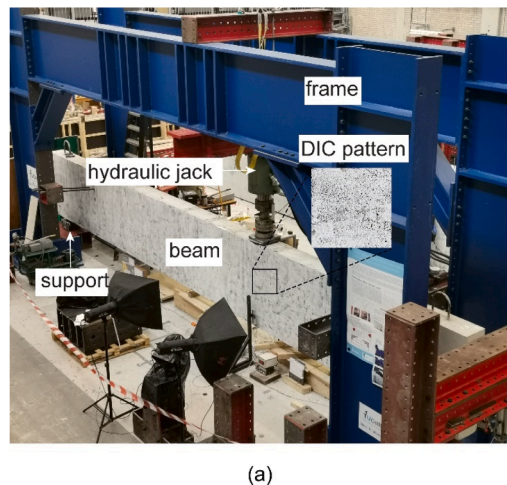
Table 2 lists the load level when the first flexural crack was observed (P_{CRI}), the load level when the critical flexural shear crack was observed ($P_{\rm u}$), the maximum load ($P_{\rm m}$) and the failure mode of the tests. The failure mode includes flexural shear failure (FS) and shear compression failure (SC). In a flexural shear failure, the specimen failed at formation of a critical flexural shear crack ($P_{\rm m}=P_{\rm u}$). For shear compression failure, after formation of critical flexural shear crack, compressive strut carried additional force, leading to larger failure load ($P_{\rm m}>P_{\rm u}$).

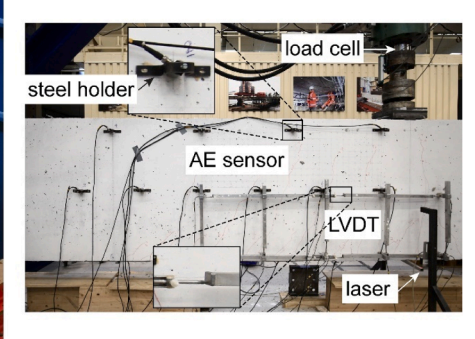
Fig. 6 also includes the crack patterns at failure, observed from one side of the beams. The major cracks are numbered from CR1 to CRn according to their opening sequence. Generally, cracks first appeared at the cross section with the largest bending moments; therefore, the crack number increased from the load side to the support side. Cracks that were outside the AE measuring zone are not numbered. They were mostly at the other span which is not interesting for this study.

By marking the estimated strut region, we find that the integrity of the strut influenced the shear capacity. In tests H603A, H604A and H853A, the flexural shear cracks did not completely cross the width of the strut. After formation of flexural shear cracks, the compressive strut carried additional shear force, leading to shear compression failure with larger shear capacity. In the other tests (H601A, H602A and I123A), the flexural shear cracks went across the complete width of the strut, leading to flexural shear failure with lower shear capacity.

5.2. Performance of the 'traffic light system'

Fig. 7 exemplifies the evaluation of the strut integrity in test I123A. Plot (a) shows the determined region of strut and the reference region with crack pattern at failure. Plot (b) shows the evolution of the maximum pdAE in the strut region and in the reference region with increasing load. Plot (c) shows the evolution of the pdAE field with the increase of load levels.





(b)

Fig. 5. Photos of the tests on reinforced concrete beams: (a) test setup including frame, hydraulic jack, support and one side of the beam with DIC pattern and (b) applied sensors on the other side of the beam including the load cell, AE sensor, LVDT and laser.

Table 1Test configurations.

Test no.	H601A	H602A	H603A	H604A	H853A	I123A
$f_{ m c.cube}$	86.40	86.08	86.08	86.08	82.99	78.24
[26]						
Age [d]	31	38	46	66	86	85
Rebar	4Ø25	4Ø25	4Ø25	4Ø25	6Ø25	8Ø25
Config.	Ribbed	Ribbed	Ribbed	Ribbed	Ribbed	Plain
f _{yk} [26]	500	500	500	500	500	240
ρ_1 [%]	0.57	0.57	0.57	0.57	0.85	1.14
a [mm]	4500	4500	3000	3500	3000	3000
d [mm]	1158	1158	1158	1158	1150	1150
a/d [-]	3.89	3.89	2.59	3.02	2.61	2.61
Load	Cyclic	Monotonic	Cyclic	Cyclic	Cyclic	Cyclic
type						

AE reference shows cracking activities in the tensile chord at 180 kN (with pdAE of $3950~\text{m}^{-3}$). This was the load level when CR2 first opened. We set the cracking threshold to be $3950~\text{mm}^{-3}$ in this test. Afterwards, the AE reference increased and stabilized at around $10,000~\text{m}^{-3}$. This met our expectation that further crack opening generated limited AE events, because the crack faces hardly made contact.

According to the 'traffic light system', the three criteria were reached at load levels of $180\ kN$, $250\ kN$ and $290\ kN$ respectively. At red-light criterion ($290\ kN$), we observed a significantly increase of AE events. This was due to the friction between the two crack faces induced by the large shear displacement near failure.

Fig. 9 shows the traffic light criteria applied in the six shear tests of reinforced concrete beams without shear reinforcement. The plots on the right-hand side show the three criteria per test. The plots on the left-hand side show the corresponding cracking behaviour in the strut and reference region. The cracking behaviour at the criteria generally meets our descriptions in Section 4. For tests failed in shear compression

Table 2
Cracking load and failure mode.

Test no.	P _{CR1} (kN)	P _u (kN)	P_{m} (kN)	Failure mode*
H601A	145	306	306	FS
H602A	125	306	306	FS
H603A	150	271	589	SC
H604A	150	251	445	SC
H853A	175	273	500	SC
I123A	170	300	300	FS

FS represents flexural shear failure, SC represents shear compression

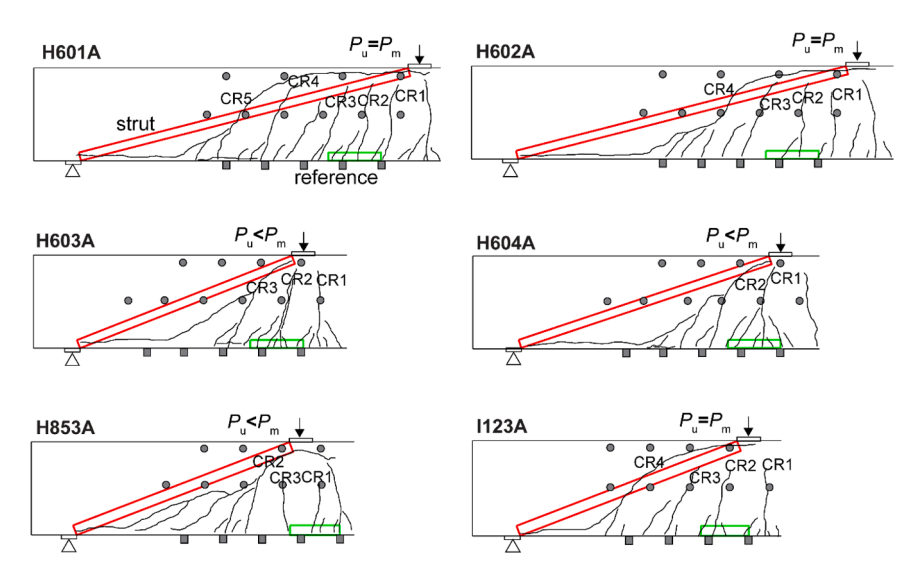


Fig. 6. Relative location between observed crack patterns and estimated compressive strut in beam tests.

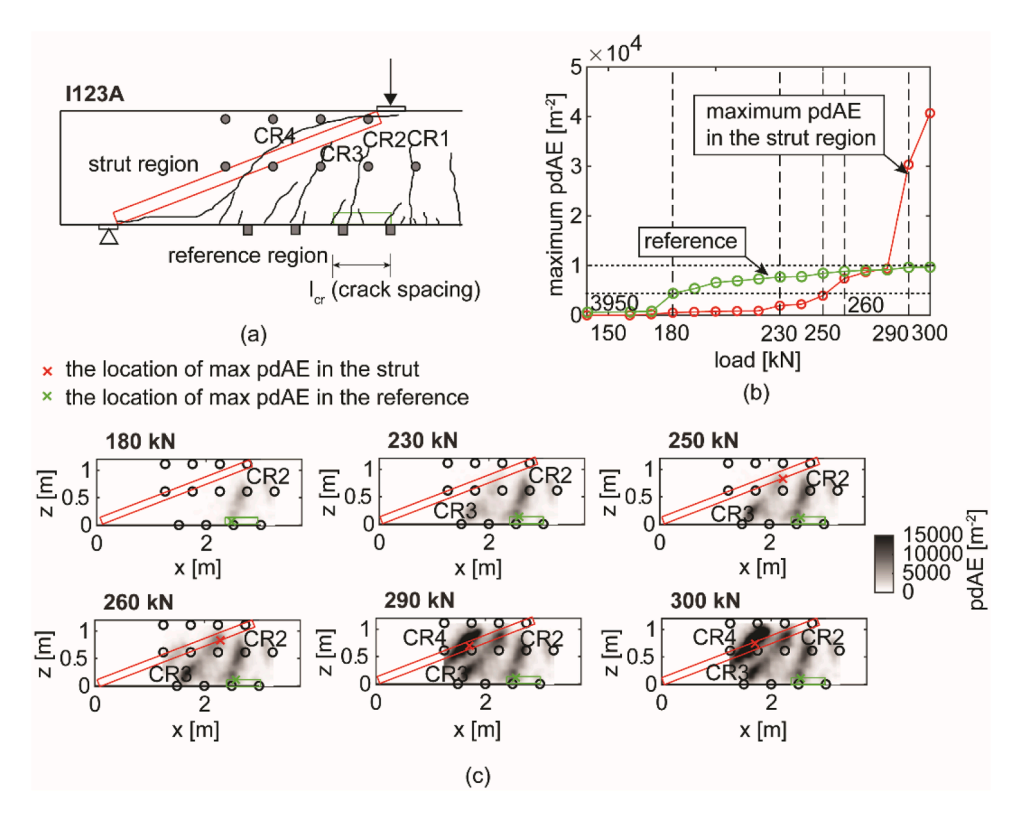


Fig. 7. Evaluation of compressive strut integrity using the maximum pdAE in I123A: (a) region of the strut and the reference region, (b) maximum pdAE in the strut region and the reference with increasing load, (c) pdAE field at the selected load levels, with the locations of the maximum pdAE in the strut and reference marked.

(H603A, H604A and H853A), the critical flexural shear crack reached the strut but did not propagate across it, thus the remaining strut provided additional shear force after the formation of the flexural shear crack (which are greyed out in Fig. 9). When the beam failed in shear compression, resulting the maximum load level ($P_{\rm m}$) larger than $P_{\rm u}$. We consider the ultimate shear capacity $P_{\rm u}$ critical, since it is not always known beforehand whether the strut can carry additional force after critical flexural shear cracking.

Table 3 lists the ratio between the load levels when a criterion is reached and the load level when shear failure was obtained in the tests. The values of $P_{\rm u}$ can be found in Table 2. $P_{\rm 1}$, $P_{\rm 2}$ and $P_{\rm 3}$ are the load level where green-light, yellow-light and red-light criteria are fulfilled respectively. The ratio between shear span a (distance between the centre of load and support) and effective height of cross section d is also listed.

The green-light criterion indicates a safe condition, with the load ratio in range of 44 %-60 %. This is reasonable as only flexural cracks form at this stage. The yellow-light criterion is fulfilled at load ratio in range of 49 %-87 %. Within the presented tests, the load ratio at yellow-light follows a certain relationship with the shear span to depth ratio (Fig. 8). With a larger shear span to depth ratio, the load ratio at yellow-light reduces. The red-light criterion could indicate a dangerous situation for flexural shear failure, with two out of six tests reaching 90 % of

Table 3Load ratio at the three criteria in the beam tests.

Beam test	a/d [-]	$P_1/P_{\rm u}$ (greenlight)	$P_2/P_{\rm u}$ (yellow-light)	$P_3/P_{\rm u}$ (redlight)
I123A	2,61	0,6	0,87	0,93
H601A	3,89	0,46	0,56	0,82
H602A	3,89	0,44	0,49	0,53
H603A	2,59	0,46	0,74	0,85
H604A	3,02	0,6	0,76	0,99
H853A	2,61	0,55	0,73	0,73

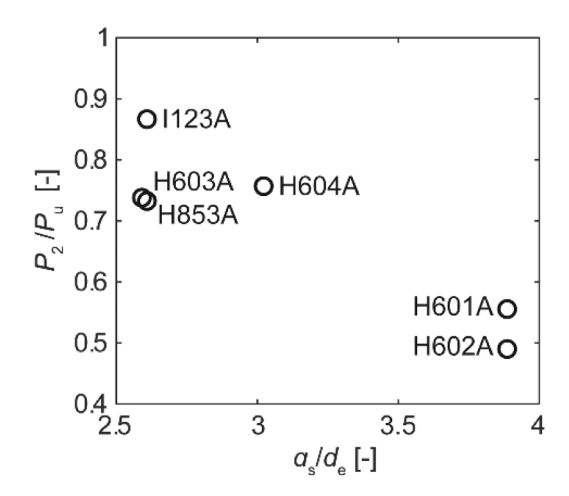


Fig. 8. Relationship between load ratio at the yellow-light criterion and shear span to depth ratio.

the ultimate shear capacity. Additional experiments are needed to more accurately characterize the distribution of the load ratio, including the mean value and standard deviation. Fig. 9

The proposed 'traffic light system' has been implemented in the workflow of the commercial AE monitoring system AEwin provided by Mistras and it could also be implemented in any other similar system. In a monitoring session like the ones presented in this paper, the indicator maximum pdAE can be updated nearly real-time when new AE events are measured. For example, in a load step of $200-225 \, \text{kN}$ in test H602A, the computational time required to calculate the pdAE field and the traffic light criteria using the detected 849,939 AE signals was 197 seconds. This calculation was performed using Matlab with the code provided in Gitlab [32]. With a more efficient programming language, such as C or C++, the computing time could be further optimized,

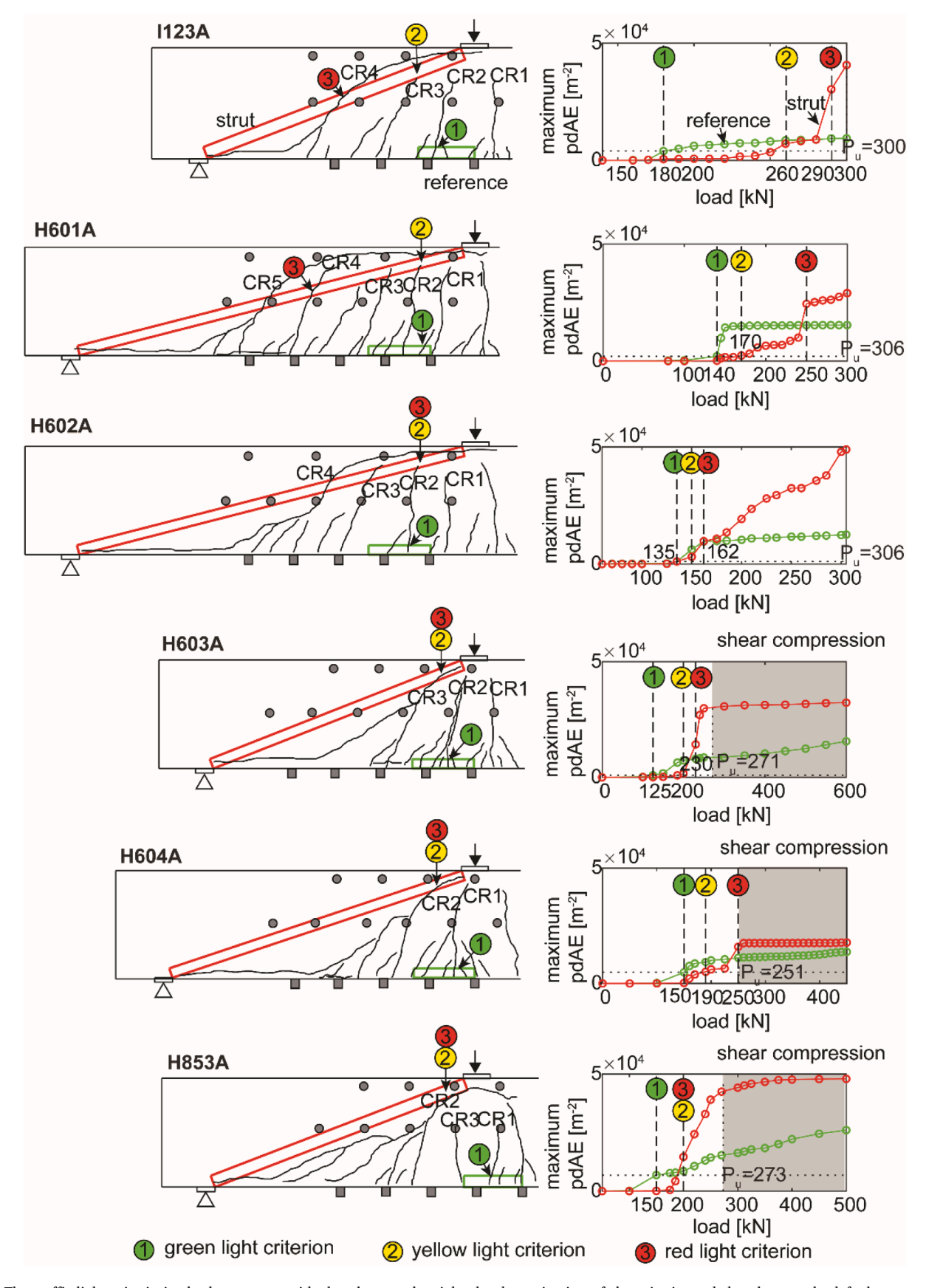


Fig. 9. The traffic-light criteria in the beam tests, with the plots on the right the determination of the criteria, and the plots on the left the corresponding cracking behaviour.

making the system even more suitable for real-time monitoring.

5.3. Robustness of the 'traffic light system'

The 'traffic light system' relies on the maximum pdAE to determine the three structural damage levels before shear failure in reinforced concrete beams without shear reinforcement. This parameter can be influences by many factors such as the variation of the crack profile locally.

The local crack profiles are in various angles to the crack opening direction. Irrespective to the global crack direction, locally, the crack profile direction may not be in line with the global crack direction (Fig. 10). In this case, the different local crack kinematic will lead to variation of pdAE value.

We evaluate the variation of the pdAE in the reference region and the strut from experiments. The variation is described by the standard deviation of pdAE at a given crack width. Fig. 11 shows the distribution and standard deviation of pdAE at several selected crack widths in a range of 0.2 – 0.8 mm. These measurements of pdAE and crack widths were taken at various locations along different cracks across the six beams. The specific measurement locations are detailed in the previous paper [25]. For Type I, we take the mean of standard deviations at these crack widths which is 1171 $\rm m^{-2}$, denoted as $\sigma_{\rm II}$. For Type II, we take the standard deviation at crack width 0.2 mm which is 3160 $\rm m^{-2}$, denoted as $\sigma_{\rm II}$. The standard deviation at other crack widths is not considered for Type II due to shortage of data.

The variation of the pdAE will influence the criteria, as shown in Fig. 12 for test I123A. Plot (a) shows the criteria without considering the variation of the measurement. while plots (b) and (c) illustrate possible situations where the variation is over- or underestimated. In these cases, the yellow-light criterion is reached at different load levels.

Using the same method, Table 4 calculates the load ratios when the three criteria are fulfilled in all the tests, taking into account the variations. The load levels that are influenced by the variation are denoted as P'_1 , P'_2 and P'_3 for green-light, yellow-light and red-light criteria respectively. The influences on green-light criterion are limited, with the load ratio increasing from 0.46 to 0.55 at the maximum (in test H603A). The influences on the red-light criterion are generally acceptable because most changes leaning towards the safe side. The influences on the yellow-light criterion are acceptable except for test H604A, where the corresponding load ratio increases from 0.76 to 0.99, which is considered unsafe.

Other uncertainties, such as the spatial variation of concrete quality, may also influence the pdAE and the criteria. Generally, at locations with lower concrete quality, AE signals are more attenuated, resulting in fewer detected AE events. Further research and testing can help refine the system, accounting for uncertainties and improving its applicability in real-world scenarios.

6. Discussion on application and future work

6.1. Suggestion on application

The three criteria in the 'traffic light system' indicate three levels of structural damage, which can support structural assessment and interventions regarding the target structure. Since the criteria are

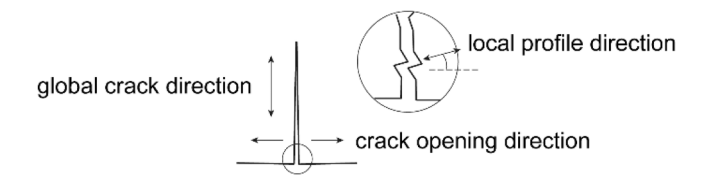


Fig. 10. Illustrated directions of crack opening, global crack pattern and local crack profile.

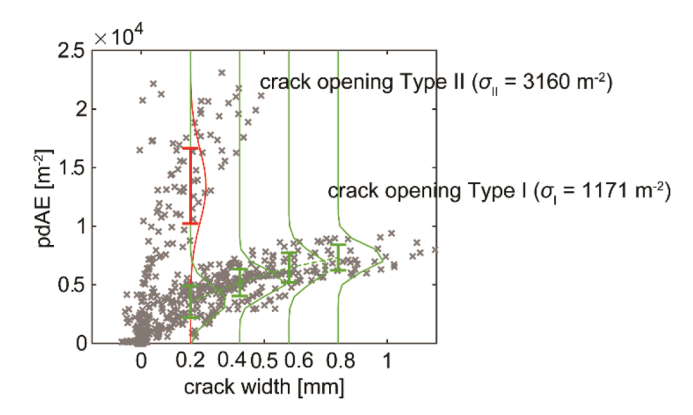


Fig. 11. Distribution of the pdAE at some selected crack widths.

calculated time-efficiently, near real-time decision-making is possible. Depending on the objectives of the users, we suggest the following actions:

- If the objective is to estimate the first cracking load, the green-light criterion should be used, which indicates the first cracking in the reference region. Users can repair the cracks afterwards.
- If the objective is to check the safety of the structure against shear failure, the yellow-light criterion should be used, which indicates the first cracking in the strut. The structure can still be used under lower load levels or be maintained to prolong its service life.
- If the objective is to get the actual shear capacity but avoid the
 collapsing of the structure, the red-light criterion should be used,
 which indicates critical cracking in the strut. But it should be noted
 that the structure is very close to failure at this criterion. The bridge
 should be closed immediately, and safety measures should be taken
 against collapse. Users can replace or repair according to the need.

Applying the 'traffic light system' to existing concrete structures requires information on the presence of existing cracks. These cracks can be identified through visual inspection or techniques such as Ultrasonic Pulse Velocity (UPV). Alternatively, a small load can be applied to the structure and then removed. During unloading, existing cracks will close and generate AE events. By localizing these AE events, the locations of existing cracks, especially internal ones within the strut, can be identified [33]. Based on the existing crack patterns, the damage condition of the strut and the level of criteria met in the structural past service life can be determined, allowing for appropriate actions to be taken.

Moreover, selecting a reference region in existing structures differs from the approach in new structures due to existing cracks. If flexural cracks have already developed in some areas, the reference should be chosen in an uncracked region as close as possible to sections with maximum bending moments to allow for earlier detection of new flexural cracks. In this case, the detected flexural cracks will not be among the first few cracks in the structure. According to the findings of this study, selecting a different flexural crack as a reference will not significantly affect the performance of the traffic light criteria (Fig. 11 and Table 4).

The 'traffic light system' was designed to enable automated determination of the three criteria. A key component of this system is the threshold indicating when a flexural crack initiates in the reference region (the green-light criterion), which also informs the yellow-light criterion. This threshold is currently identified by an obvious increase in pdAE in the reference region. However, setting a fixed value for this 'obvious increase' is challenging due to differences in AE setup and material properties across tests. An alternative approach could involve establishing a fixed pdAE threshold based on the pdAE-crack width relationship for Type I cracks in Fig. 3a. This approach equals to setting a crack width threshold to indicate crack initiation. However, this pdAE-

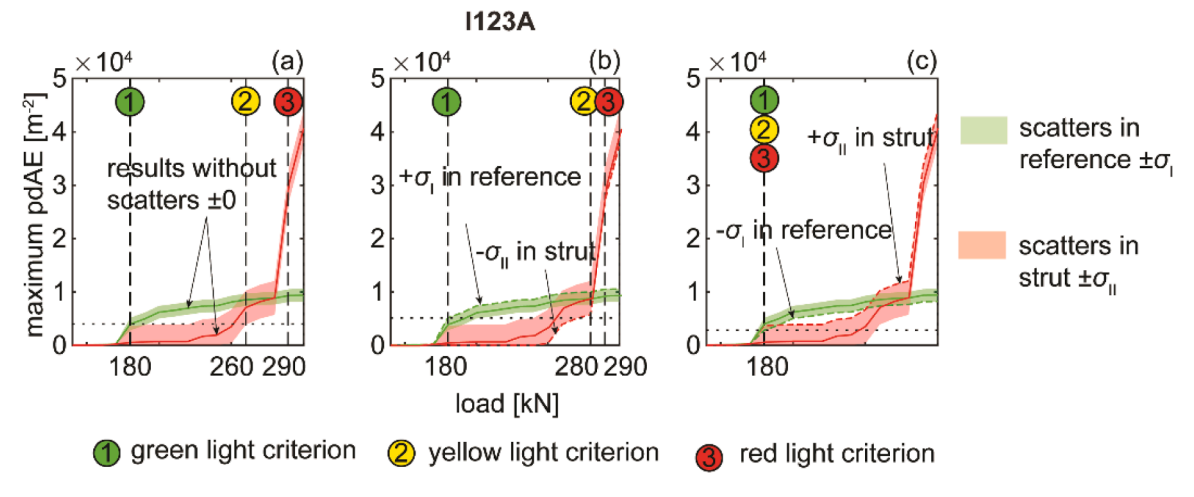


Fig. 12. Influence of scattering on traffic light criteria in test I123A: (a) without scattering, (b) overestimating an σ_I in the reference and underestimating an σ_I in the strut, and (c) underestimating an σ_I in the reference and overestimating an σ_I in the strut.

Table 4Load ratio at the traffic light criteria in beam tests, influenced by the variation of the crack pattern.

	Green-light criterion		Yellow-light criterion		Red-light criterion	
Beam test	$P_1/P_{\rm u}$	$P'_1/P_{\rm u}$	$P_2/P_{\rm u}$	$P'_2/P_{\rm u}$	$P_3/P_{\rm u}$	$P'_3/P_{\rm u}$
I123A	0.6	0.6	0.87	0.6-0.93	0.93	0.6 - 0.97
H601A	0.46	0.46	0.56	0.47-0.65	0.82	0.82
H602A	0.44	0.44-0.49	0.44	0.49-0.53	0.53	0.49-0.65
H603A	0.46	0.46-0.55	0.74	0.68 - 0.85	0.85	0.85
H604A	0.6	0.6	0.76	0.64-0.99	0.99	0.76-0.99
H853A	0.55	0.55	0.73	0.68 - 0.73	0.73	0.68 - 0.73

crack width relationship also needs verification across different tests. Without sufficient verification, expert judgment may initially be needed to establish the green-light criterion, after which the system can function automatically.

6.2. Future work

To allow broader application of the 'traffic light system', further development is suggested in the following perspectives. First, the dependence of the yellow-light criterion on the shear span and depth ratio needs to be further studied with more tests. In these tests, both the dependency and associated uncertainties will be examined. Additionally, the underlying reasons for the observed relationships should be further clarified.

Second, the robustness of the 'traffic light system' is now only validated in laboratory conditions, more demonstrations in real structures are needed to ultimately validate the system. For monitoring real structures, factors such as sensor protection and weather changes need to be considered.

Third, the system can be extended to monitor other type of reinforced concrete structures without shear reinforcement under different loading conditions. The region of strut and reference can be determined according to the stress distribution. For instance, in the case of a distributed load, a fan-shaped strut region can be estimated [34]. And in the case of members with larger width, such as slabs, 3D AE monitoring is required, and the 3D strut region needs be determined. Then, a same methodology can then be used: comparing the maximum pdAE in the strut to that in the reference, to indicate the integrity of the strut which is closely related to the shear failure of the structure. The extension to another type of structure, reinforced concrete slab, is presented in a subsequent paper.

7. Conclusion

This paper presents AE-based indicators for shear failure of reinforced concrete structures without shear reinforcement. For this type of structure, the compressive strut is unreinforced, thus suffers from brittle failure. Failure of the strut would lead to the flexural shear failure of the structure. Therefore, evaluation of the integrity of the strut along the shortest load transfer path between loading point and support as an indicator to shear failure.

To evaluate the integrity of the strut, we used the maximum pdAE in the strut which is compared to the maximum pdAE in the reference region. The selection of strut and reference region was according to a typical strut and tie model: a prismatic compressive strut was assumed between the load and the support; and a reference region was selected within the tension chord where the flexural cracks form.

Based on the evaluation of the strut integrity, we proposed a 'traffic light system' which indicates three levels of structural degradation against flexural shear failure: the green-light criterion corresponds to the first formation of flexural crack; the yellow-light criterion corresponds to the initiation of cracking damage in the compressive strut; the redlight criterion corresponds to the situation that a critical flexural shear crack propagated across/along the strut, which was close to the flexural shear failure.

The traffic light system is validated with a set of six large scale shear tests. In the validation, the green-light criterion was reached at load level 44 %-60 % of the shear capacity. The yellow-light criterion was reached at load ratio in range of 49 %-87 %, related to the shear span to depth ratio. The red-light criterion indicated a very dangerous situation for flexural shear failure, with load levels close to the shear capacity. We also validated the robustness of the traffic light system to the variation of local crack profile within the presented tests.

The AE-based 'traffic light system' contributes to the field of predicting shear failure of concrete structures. Its strong physical background of using AE parameters to indicate the strut integrity, criteria to indicate the multiple levels of structural damage, applicability to different structures, and computational efficiency of calculating AE parameters make it a promising tool for future applications in structural assessment of reinforced concrete structures without shear reinforcement.

Funding

This work was partly supported by Rijkswaterstaat, the Netherlands.

CRediT authorship contribution statement

Zhang Fengqiao: Writing – review & editing, Writing – original draft, Visualization, Validation, Software, Methodology, Investigation, Formal analysis, Data curation, Conceptualization. Yang Yuguang: Writing – review & editing, Supervision, Resources, Funding acquisition, Conceptualization. Hendriks Max A.N.: Writing – review & editing, Supervision, Resources, Conceptualization.

Declaration of Competing Interest

The authors declare the following financial interests/personal relationships which may be considered as potential competing interests: Fengqiao Zhang reports financial support was provided by Rijkswaterstaat. If there are other authors, they declare that they have no known competing financial interests or personal relationships that could have appeared to influence the work reported in this paper.

Data availability

The Matlab code to calculate the AE-based shear failure indicators is shared in https://gitlab.tudelft.nl/fzhang9/fengqiao-zhang-phd-project.

References

- [1] Fischer, O., et al., 2016. Nachrechnung von Betonbrücken Systematische Datenauswertung nachgerechneter Bauwerke Re-analysis of concrete bridges " systematic data evaluation of re-analysed concrete bridges. Berichte der Bundesanstalt für Straßenwesen, Reihe B: Brücken- und Ingenieurbau - 124.
- [2] Rijkswaterstaat, Staat van de Infra. 2021.
- [3] Lantsoght EOL, et al. Recommendations for the shear assessment of reinforced concrete slab bridges from experiments. Struct Eng Int 2013;23(4):418–26.
- [4] Anderson BG. Rigid frame failures. Acids J 1957;53(1):625-36.
- [5] Lantsoght EOL. Load Testing of Bridges: Two. 1 ed., Set. CRC Press; 2019. p. 346.
- [6] fib, Monitoring and safety evaluation of existing concrete structures. fib bulletin. Vol. 22, 2003: Elsener and Böhni. 297.
- [7] Zararis PD, Papadakis GC. Diagonal shear failure and size effect in rc beams without web reinforcement. J Struct Eng 2001;127(7):733–42.
- [8] Tue NV, Theiler W, Tung ND. Schubverhalten von Biegebauteilen ohne Querkraftbewehrung. Beton- Stahlbetonbau 2014;109(10):666–77.
- [9] Muttoni, A. and M. Fernández Ruiz Shear strength of members without transverse reinforcement as function of critical shear crack width. 2008. 105, No 2, 163-172-163-172.
- [10] Yang Y, den Uijl J, Walraven J. Critical shear displacement theory: on the way to extending the scope of shear design and assessment for members without shear reinforcement. Struct Concr 2016;17(5):790–8.

- [11] Reineck K-H. Ultimate shear force of structural concrete members Without Transverse Reinforcement Derived From a Mechanical Model (SP-885). Acids Struct. J 1991:88(5).
- [12] Hoffmann K. An introduction to measurements using strain gages. Hottinger Baldwin Messtechnik Darmstadt; 1989.
- [13] Jones, E., Documentation for Matlab-based DIC code. 2015: Urbana-Champaign: University of Illinois.
- [14] Soga K, Luo L. Distributed fiber optics sensors for civil engineering infrastructure sensing. J Struct Integr Maint 2018;3(1):1–21.
- [15] McCann DM, Forde MC. Review of NDT methods in the assessment of concrete and masonry structures. NDT E Int 2001;34(2):71–84.
- [16] Soutsos, M., et al., Non-Destructive Assessment of Concrete Structures: Reliability and Limits of Single and Combined Techniques. 2012. p. 119-186.
- [17] Chateau C, et al. In situ X-ray microtomography characterization of damage in SiCf/SiC minicomposites. Compos Sci Technol 2011;71(6):916–24.
- [18] Pahlavan L, et al. Interaction of ultrasonic waves with partially-closed cracks in concrete structures. Constr Build Mater 2018;167:899–906.
- [19] Martin J, Forde MC. Influence of concrete age and mix design on impulse hammer spectrum and compression wave velocity. Constr Build Mater 1995;9(4):245–55 (p. n.).
- [20] Grosse C., Ohtsu M. 2008. Acoustic emission testing: Basics for Research-Applications in Civil Engineering, 1-404.
- [21] Grosse C, et al. Acoustic emission testing: Basics for Research-Applications in Engineering. 2 ed. Springer Tracts in Civil Engineering. Switzerland: Springer Cham. X; 2021. p. 752.
- [22] Leonhardt F, Walther R. Shear tests on beams with and without shear reinforcement. Dtsch Aussch FüR Stahlbeton 1962;(151):83.
- [23] Kundu T. Acoustic source localization. Ultrasonics 2014;54(1):25-38.
- [24] Zhang F, et al. Probability density field of acoustic emission events: Damage identification in concrete structures. Constr Build Mater 2022;327:126984.
- [25] Zhang F, Yang Y, Hendriks MAN. Investigation of concrete crack kinematics through probability density field of the location of acoustic emission events. Constr Build Mater 2023;400:132595.
- [26] Muttoni A, et al. Analysis of shear-transfer actions on one-way RC members based on measured cracking pattern and failure kinematics. Mag Concr Res 2013;65: 386–404.
- [27] Yang, Y., et al., Calibration of the shear stop criteria based on crack kinematics of reinforced concrete beams without shear reinforcement, in fib Congress. 2018: Melbourne. Australia.
- [28] Yang Y. Shear Behaviour of Reinforced Concrete Members without Shear Reinforcement, Delft, the Netherlands; Delft University of Technology; 2014.
- [29] Yang Y. Shear behaviour of deep RC slab strips (beams) with low reinforcement ratio. Stevin Report. Delft, the Netherlands: Delft University of Technology; 2020.
- [30] MISTRASR6I-AST Sensor, in Product Data Sheet. 2008, MISTRAS Group Inc.: Princeton Junction. NJ 08550..
- [31] MOLYKOTEMOLYKOTE 4 Electrical Insulating Compound, in Product Data Sheet. 2018. DuPont de Nemours. Inc.2018.
- [32] Zhang F. 2022. Matlab codes for PhD thesis acoustic emission-based indicators of shear failure of reinforced concrete structures without shear reinforcement, (htt
- [33] Zhang F., Yang Y. 2019. Acoustic Emission based Crack Tracking for Concrete Structures.

ns://gitlab.tudelft.nl/fzhang9/fenggiao-zhang-phd-project).

[34] Schlaich J, Schäfer K, Jennewein M. Toward a consistent design of structural concrete. PCI J 1987;32(3):74–150.